CHEMISTRY OF MATERIALS
Cite This: Chem. Mater. XXXX, XXX, XXX−XXX
Article
pubs.acs.org/cm

Breaking the Bimolecular Crystal: The Effect of Side-Chain Length on Oligothiophene/Fullerene Intercalation

Edmund K. Burnett,[†,#] Benjamin P. Cherniawski,[†,#] Stephen J. Rosa,[†] Detlef-M. Smilgies,[‡] Sean Parkin,[§] and Alejandro L. Briseno*[,†]

[†]Polymer Science and Engineering, University of Massachusetts Amherst, 120 Governors Drive, Amherst, Massachusetts 01003, United States

[‡]Cornell High Energy Synchrotron Source, Cornell University, Ithaca, New York 14850, United States

[§]Department of Chemistry, University of Kentucky, Lexington, Kentucky 40506-005, United States

Supporting Information

ABSTRACT: Polymer/fullerene bimolecular crystal formation has been investigated using a variety of conjugated polymers and fullerenes to understand the design rules that influence donor−acceptor interaction. Modifications of the polymer by varying the substitution side-chain position, density, and branching have demonstrated the importance of the "pocket" dimensions (free volume between side chains where the fullerene resides) for controlling intercalation. Yet the effect of pocket height has not been systematically explored because of the solubility limitations in polymers. In this report, we present an experimental investigation into the effect of the pocket height by synthesizing poly[2,5-bis(3-*alkyl*thiophen-2-yl)thieno[3,2-*b*]thiophene] dimers with varied side chain lengths and track the morphological changes of the dimer/fullerene blends using grazing-incidence X-ray scattering, thermal measurements, and photoluminescence quenching. We identify two regimes: (1) oligomers with side chains greater than or equal to heptyl (C7) form bimolecular crystals and (2) oligomers with less than or equal to hexyl (C6) form amorphous blends. This work provides the first observation of an order-to-disorder transition mediated by side-chain length in donor-fullerene intercalated blends.

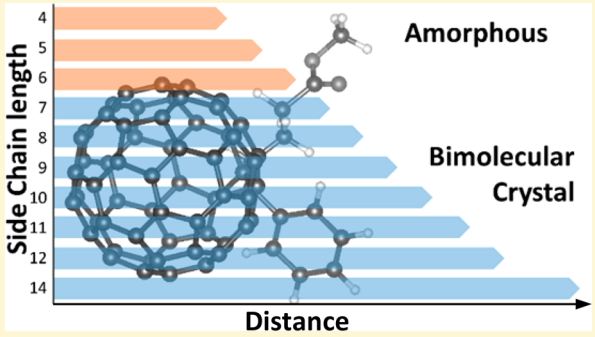

Morphology and microstructural control is essential for efficient organic photovoltaic (OPV) devices.[1−4] Short exciton diffusion lengths in organic semiconductors require careful tuning of domain spacing and purity for efficient charge generation.[5,6] The bulk heterojunction (BHJ) morphology is a widely adopted strategy to maximize interfacial surface area while maintaining desirable domain spacings.[7,8] It was originally assumed that the donor and acceptor phases were pure, yet there has been experimental evidence of amorphous mixed phases,[9−13] and even certain morphologies in which fullerenes intercalate within polymer side chains.[14−20]

Fullerene intercalation has been observed to form both amorphous[20] and crystalline phases;[14,19] intercalated crystalline phases are defined as bimolecular crystals. While intimate mixing of donors and acceptors is detrimental to OPV performance, polymer/fullerene intercalated systems have provided valuable insight into fundamental OPV processes.[21−24] Recently, Banerji and co-workers used poly[2,5-bis(3-*alkyl*thiophen-2-yl)thieno[3,2-*b*]thiophene] (PBTTT) and fullerene bimolecular crystals to better understand charge separation and recombination physics at the donor−acceptor interface.[25] In general, intercalation provides a powerful approach for the inclusion of small molecules without disrupting microstructure, and has shown promise in doped polymer systems.[26]

Reports investigating the design rules for bimolecular crystal formation reveal that fullerene chemistry and side-chain type and spacing influence intercalation.[14,17,18] Fullerenes with or without solubilizing groups are observed to intercalate with compatible polymers. With additional substitutions, the fullerene becomes too bulky to intercalate and phase separation is observed instead.[18] Steric limitations can also be imposed by side chains. For all intercalating polymers, the side-chain substitution pattern along the backbone must offer sufficient space to accommodate a fullerene.[14] This space, called the "pocket", has been modulated by varying the substitution position, density, and side-chain branching.[14] Yet, the effect of the pocket height (modulated by side-chain length) has not been explored because of solubility limitations in polymers with decreasing side-chain length. Oligomers, which exhibit shared properties of the corresponding polymer, provide a versatile experimental platform unhindered by the solubility issues that

Received: November 9, 2017
Revised: March 24, 2018
Published: March 26, 2018

DOI: 10.1021/acs.chemmater.7b04702
Chem. Mater. XXXX, XXX, XXX−XXX

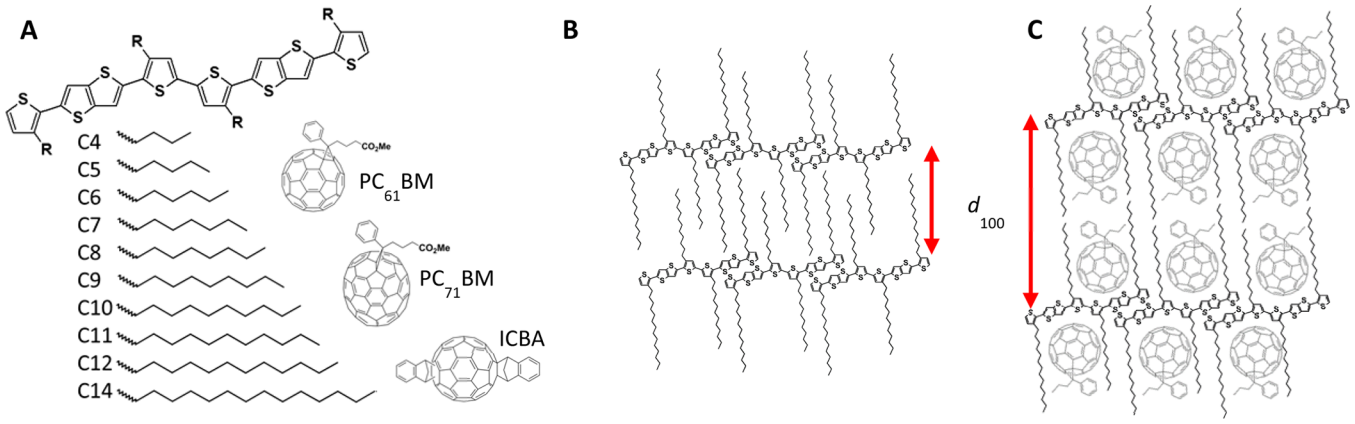

Figure 1. (A) Chemical structure of BTTT-R dimers and selected side chain series. Cartoon representations of (B) neat dimer interdigitation in the solid-state and (C) the intercalated BTTT-R/fullerene bimolecular crystal.

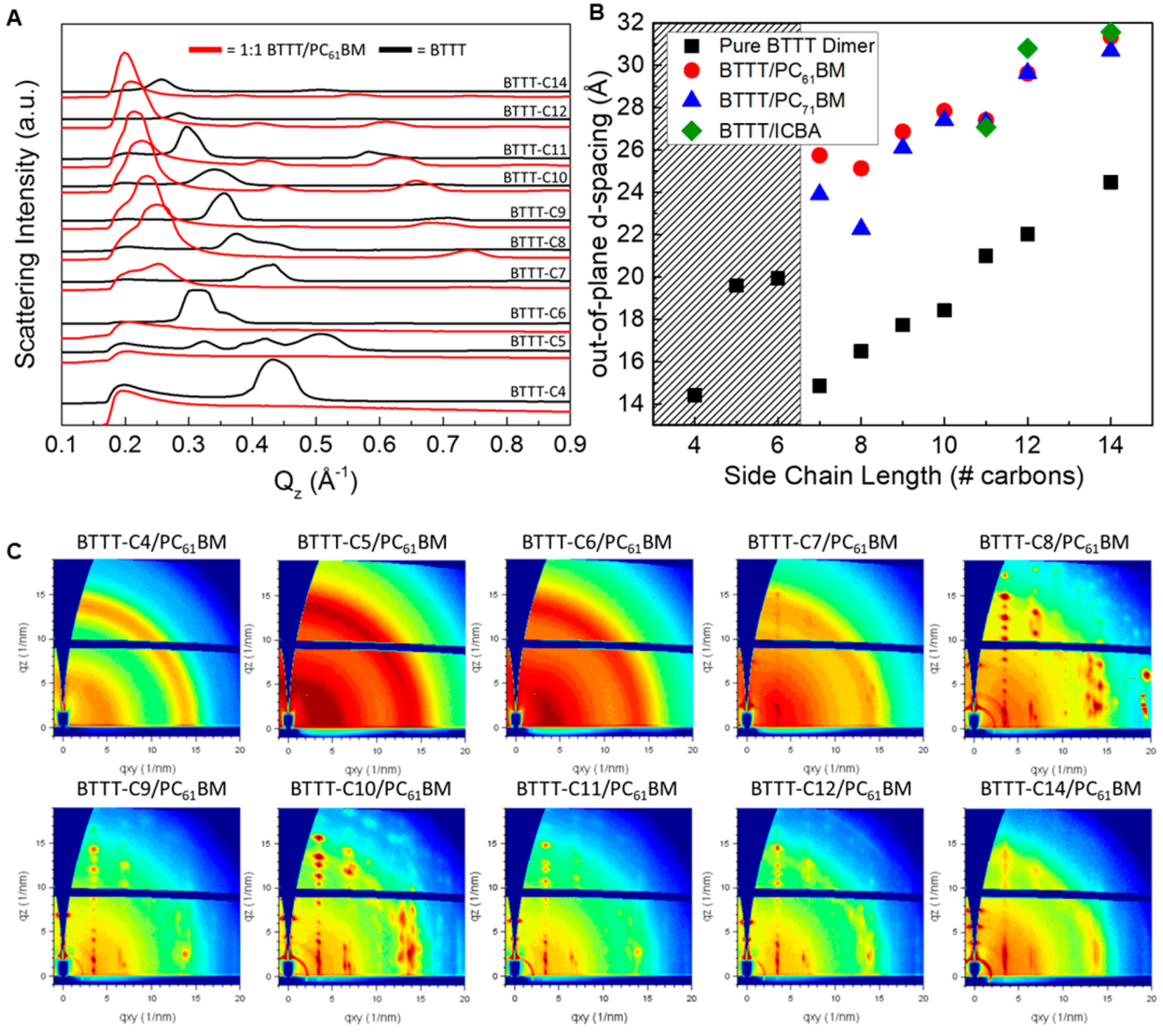

Figure 2. (A) GIXD Q_z line cuts of neat dimer films (black) and $PC_{61}BM$/dimer blended (1:1 wt %) films. (B) Lamellar *d*-spacing as a function of side chain length for neat films (black, square), $PC_{61}BM$ blended films (red, circle), $PC_{71}BM$ blended films (blue, triangle), and ICBA blended films (green, diamond). Line fill indicates amorphous blends without bimolecular crystal formation. (C) Diffraction patterns of the BTTT dimers blended with $PC_{61}BM$.

DOI: 10.1021/acs.chemmater.7b04702
Chem. Mater. XXXX, XXX, XXX−XXX

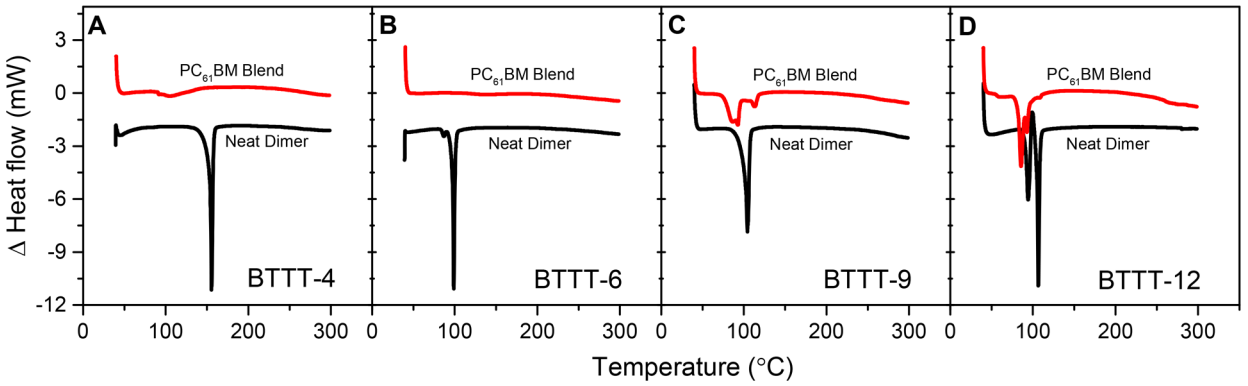

Figure 3. Differential scanning calorimetry first heating curves of neat dimers (black) and 50:50 wt % blends with $PC_{61}BM$ (red) of (A) BTTT-4, (B) BTTT-6, (C) BTTT-9, and (D) BTTT-12. Exo up.

limit systematic polymer studies. The benchmark polymer, PBTTT, is known to intercalate with fullerenes, and we previously demonstrated PBTTT-oligomers also form a bimolecular crystal with fullerenes.[27] To systematically study the effect of side chain length on bimolecular crystal formation, we synthesized BTTT dimers with linear alkyl side chains from butyl (C4) to tetradecyl (C14) and blend them with three fullerene derivatives varying in size and substitution (Figure 1A). Grazing-incidence X-ray diffraction (GIXD) reveals a transition from a bimolecular crystal to an intimately mixed amorphous blend upon decreasing side chain length. We further characterize these oligomer/fullerene blends using differential scanning calorimetry (DSC) and photoluminescence spectroscopy (PL) to understand this transition and probe the newly observed amorphous phase.

Detailed synthesis is described in the Supporting Information and the general procedure has been previously reported.[27,28] Briefly, 3-*alkyl*thiophenes were synthesized through Kumada coupling of alkyl Grignards and 3-bromothiophene. The 2-position of the thiophene was selectivity brominated with NBS to afford 2-bromo-3-*alkyl*thiophene. Stille coupling of 2-bromo-3-alkylthiophene and 2,5-bis(trimethyltin)-thieno[3,2-*b*]-thiophene yielded the BTTT monomer. The monomer is monobrominated with NBS and purified prior to Stille coupling with hexamethylditin to afford the final product. Precursors and final products were purified with column chromatography (silica gel) in hexanes. We selected [6,6]-phenyl-C_{61}-butyric acid methyl ester ($PC_{61}BM$), its C_{70} analogue ($PC_{71}BM$), and indene-C_{60}-bisadduct (ICBA) fullerenes to explore variations in size and substitution. Chemical structures of BTTT dimers, side chains, fullerenes, and also interdigitated and intercalated lamellar packings are shown in Figure 1.

Intercalation of fullerenes causes an increase in the lamellar spacing of a BTTT dimer, visualized in Figure 1B,C; thus, GIXD was employed to measure the lamellar spacing of the neat and blended BTTT/fullerene films to determine if bimolecular crystal formation occurs. Samples were prepared by mixing 50:50 wt % BTTT with $PC_{61}BM$, $PC_{71}BM$, and ICBA in a heated chloroform solution and spin coating onto silicon substrates. In the neat films, the BTTT dimers pack in a manner similar to PBTTT, with the lamellar stacking axis oriented out-of-plane with side chain interdigitation.[29] Out-of-plane line cuts of the neat and blended films for all side chain lengths are shown in Figure 2A. Additional line cuts and a full set of diffractograms are located in the Supporting Information. BTTT lamellar spacing increases linearly from BTTT-7 (14.9 Å) to BTTT-14 (24.5 Å) similar to that of PBTTT films with varied side chain lengths.[30] Dimers with side chain lengths of C5 through C8 show evidence of polymorphism in neat films. When the dimers are blended with $PC_{61}BM$, a shift in the peak positions along $q_z \sim 0$ indicates an increase in lamellar spacing consistent with bimolecular crystal formation for BTTT-7/$PC_{61}BM$ (25.8 Å) through BTTT-14/$PC_{61}BM$ (31.4 Å). Note, despite evidence of multiple polymorphs in the BTTT-7 and -8 neat films, addition of fullerene unifies the morphology to a single, intercalated packing. Figure 2B shows the *d*-spacing vs side chain length in the neat and blended films.

BTTT with hexyl (C6) and shorter side chains do not follow the linear lamellar spacing trend observed for longer side chains because of a different thin-film molecular packing. Interestingly, blends of BTTT-6 and shorter with fullerenes do not show an increase in *d*-spacing; instead, the BTTT scattering intensity is completely suppressed and replaced by broad powder rings corresponding to $PC_{61}BM$, indicating a morphology of amorphous dimer and nanocrystalline PCBM. However, we contend that even at decreased pocket height, fullerenes can still occupy the space between the side chains and intercalate, disrupting aggregation and crystallization of the dimer and fullerene. In separate studies, polyterthiophene (PTT) also exhibited similar side-chain mediated behavior. McGehee and co-workers report bimolecular crystal formation in fullerene blends with PTT-C14 containing long tetradecyl side chains.[19] Yet, Scharber and co-workers reported fullerene blends with shorter hexyl side chains, PTT-C6, showing crystallization suppression also observed in our study and attributed this to fullerene intercalation.[31] These studies support our claim that BTTT dimer-fullerene blends transition from crystalline to amorphous with decreasing side chain lengths while maintaining an intercalated morphology.

Additional experiments varying fullerene size ($PC_{61}BM$ vs $PC_{71}BM$) showed no significant differences in lamellar spacing of the bimolecular crystal or transition to the amorphous blend. We do note a small deviation in lamellar spacing at side chains C7 and C8 with $PC_{71}BM$. ICBA, an alternate disubstituted fullerene known to intercalate with PBTTT, was also investigated. ICBA blends demonstrated only partial intercalation into BTTT dimers ≥C11. Additionally, blends with BTTT-11, -12, and -14 exhibit lamellar spacing corresponding to domains of both pure dimer and bimolecular crystal. Films of ICBA with BTTT-10 and shorter show suppression of the cocrystalline microstructure, mirroring PCBM blends with smaller side chains. Interestingly, the lamellar spacing of the

DOI: 10.1021/acs.chemmater.7b04702
Chem. Mater. XXXX, XXX, XXX−XXX

ICBA bimolecular crystal was very similar to the PCBM blends, differing from what has been previously reported with blends of PBTTT/ICBA, which exhibited a smaller expansion of the side chains upon the introduction of ICBA compared to PCBM derivatives.[17] This could be due to the ICBA arranging in a differing manner in which the side groups are not perpendicular to the BTTT side chains and thus contribute to the lamellar spacing of the bimolecular crystal.

To probe the order-to-disorder transition observed in GIXD, we characterized the thermal behavior of both neat and blended films of BTTT-12, -9, -6, and -4 with DSC. Figure 3 shows the first heating thermograms of the neat dimer and $PC_{61}BM$ blends. To emulate the thin-film processing conditions, 5 mg/mL chloroform solutions were drop cast directly into aluminum hermetic pans, or dried in glass vials, scraped, and then loaded. All neat materials exhibit strong melting endotherms. BTTT-6, -9, and -12 melt around 100 °C, whereas BTTT-4 melts at 155 °C. Upon blending, BTTT-12 and -9 show a melting point shift, indicating a new crystalline phase, which we attribute to the bimolecular crystal. In the blended samples of BTTT-6 and -4, the melting transition is suppressed. The absence of a strong melting endotherm in BTTT-6 and -4 support the featureless diffraction patterns and the proposed order-to-disorder transition at side chain lengths ≤C6. Full heat/cool/heat cycles of drop-cast samples, neat powders, and BTTT-4 blends with $PC_{61}BM$, $PC_{71}BM$, and ICBA are available in the Supporting Information.

PL quenching is an indicator of how efficiently excitons can diffuse to a donor−acceptor interface.[32,33] In intercalated systems, excitons are formed in immediate proximity of a fullerene, allowing for near quantitative PL quenching.[18,20] Conversely, in phase-separated systems, some population of excitons formed in the donor phase do not reach an interface and recombine emissively.[18,20−23] To gain insight into the distribution of donor and acceptor molecules within the amorphous blends, we compare the PL quenching behavior of the cocrystalline and amorphous blends. Figure 4 shows the PL signal for both neat and blended systems. Upon fullerene blending, both cocrystalline and amorphous systems demonstrated complete quenching. PL spectra of the crystalline and amorphous blends confirm no pure domains larger than the nanometer scale exist.

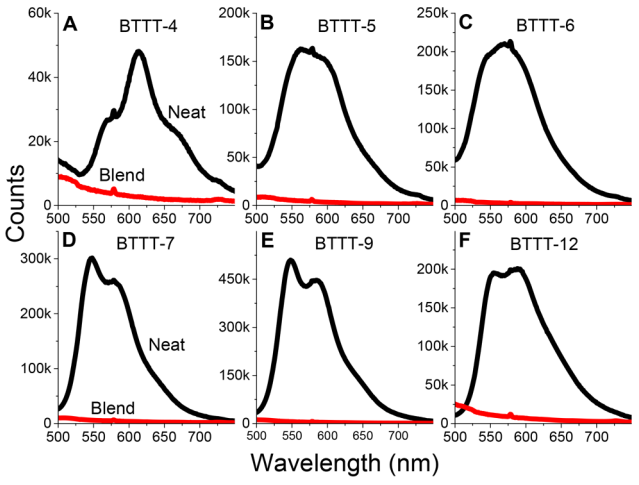

Figure 4. Photoluminescence of neat (black) and 50:50 wt % BTTT/$PC_{61}BM$ (red) films of (a) BTTT-4, (b) BTTT-5, (c) BTTT-6, (d) BTTT-7, (e) BTTT-9, and (f) BTTT-12. Excitation wavelength: 450 nm.

To correlate the morphology to the electronic properties of the bimolecular crystal and amorphous blends, electron-only, hole-only, and field-effect transistor devices were fabricated. In our previous work, we determined the structural model of the BTTT-12/$PC_{61}BM$ bimolecular crystal.[27] This packing is characterized by one-dimensional connected channels of fullerenes sandwiched between layers of two-dimensional connected dimers aligned parallel to the substrate. Because of the highly oriented nature of the cocrystal and the lack of structural information on the amorphous blend, measuring the out-of-plane (electron-/hole-only devices) and in-plane (OFET) transport builds a more complete picture of the molecular connectivity and arrangement. BTTT-6 was chosen as a representative dimer of the amorphous blend, and BTTT-12 to represent the bimolecular crystal.

Current density−voltage characteristics of the electron-only and hole-only devices are shown in parts (a) and (b), respectively, of Figure 5. Electron-only devices consisted of indium tin oxide (ITO)/C_{60}-N/active layer/Ca/Ag. The highest current density is observed in pure PCBM devices. Upon blending, current density decreases, yet electron transport in the amorphous blend of BTTT-6/$PC_{61}BM$ is greater than that of the bimolecular crystal of BTTT-12/$PC_{61}BM$. The combination of GIXD and electrical measurements indicates that amorphous blends afford greater three-dimensional connectivity of the fullerene. This is evident from the halo at $Q \sim 1.4$ Å^{-1} associated with $PC_{61}BM$ order being more prominent than that in the bimolecular crystal. In BTTT-12 devices, the bimolecular crystals orient edge-on to the substrate and cause the fullerenes to lose vertical connectivity and decrease electron transport. Hole-only devices of the dimers were fabricated using the architecture ITO/poly(3,4-ethylenedioxythiophene):poly(styrene sulfonate)/active layer/MoO_x/Ag. The current densities of the neat dimers were very similar, yet upon blending of the dimers with $PC_{61}BM$ the current in the BTTT-6/$PC_{61}BM$ blend (amorphous) was lower than that in the BTTT-12/$PC_{61}BM$ (bimolecular crystal) because of the loss of BTTT crystallinity.

To explore in-plane charge transport within these blends, bottom-gate, bottom-contact field-effect transistors were also fabricated using the same processing conditions consistent with GIXD sample preparation. The mobility of the BTTT-6 was calculated to be 2 orders of magnitude greater than that of BTTT-12 in the neat film. GIXD and DSC indicate that BTTT-6 adopts a different thin-film packing, which accounts for the improved charge transport in the neat film.[28] Upon blending of the dimers with $PC_{61}BM$, the BTTT-6/$PC_{61}BM$ device exhibited no field effect, while the BTTT-12/$PC_{61}BM$ transistor performance improved by 2 orders of magnitude. Summary of device performance is shown in Table 1.

While we are uncertain of the fundamental driving force behind the BTTT/fullerene order-to-disorder transition as mediated by side-chain length, we point interested readers to a report by Jayaraman and co-worker.[34] This work details coarse-grain morphology simulations of BTTT dimers with varying side-chain lengths and fullerene. They observed a change in the blended morphologies at the shorter side-chain length (the BTTT-C6 analog), which is in remarkable agreement with our findings.

To more directly address the underlying forces at play, we highlight a few of our results which provide critical clues. We

DOI: 10.1021/acs.chemmater.7b04702
Chem. Mater. XXXX, XXX, XXX−XXX

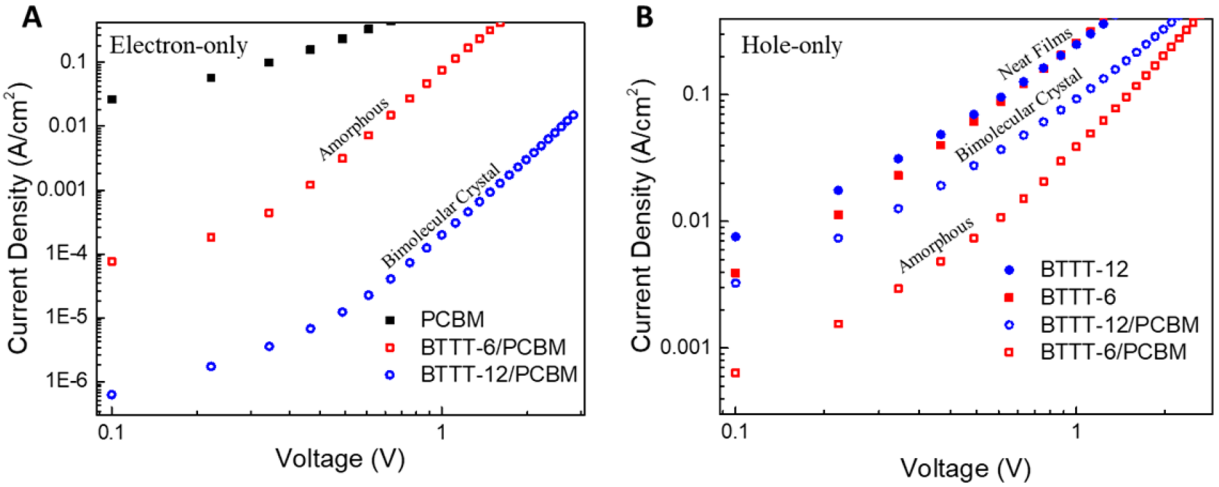

Figure 5. Current density−voltage characteristics of (a) electron-only and (b) hole-only devices comparing neat and blended films that form bimolecular crystals and amorphous blends.

Table 1. OFET Characteristics Comparing Neat and Blended Films of Bimolecular Crystals and Amorphous Blends

material	mobility ($cm^2/V{\cdot}s$)	threshold voltage (V)	on/off
BTTT-6	$(4.5 \pm 0.25) \times 10^{-4}$	24.9 ± 1.1	10^2
BTTT-12	$(1.27 \pm 0.05) \times 10^{-6}$	9.3 ± 1.0	10^2
BTTT-6/PCBM	no field effect		
BTTT-12/PCBM	$(3.0 \pm 0.1) \times 10^{-4}$	12.4 ± 0.7	10^2

observe the order-to-disorder transition of the blended system is dependent on both the side-chain length (long vs short) and fullerene chemistry (PCBM vs ICBA). ICBA did not illicit different phase behavior, but did shift the onset of the transition to larger side chain lengths. No size dependency was observed in the $PC_{61}BM$ versus $PC_{71}BM$ results, possibly because their size difference is not large enough to cause a shift. Alternatively, the molecular design, bis-adduct (ICBA) versus the mono-adduct ($PC_{61/71}BM$), could have a larger effect than fullerene size alone.

Regardless of fullerene size/type, small side chains (≤C6) do not fully envelope the fullerene and solubilizing group within the pocket. This allows fullerenes to establish additional nonbonding interactions which likely contribute to the amorphous microstructure formation. This curious and reproducible microstructure, which is conserved across multiple fullerenes unambiguously indicates that BTTT and fullerene interact significantly, even at "undersized" pocket dimensions.

In summary, we investigated the effect of side-chain length on the formation of BTTT/fullerene bimolecular crystals. BTTT dimers with alkyl side-chain lengths ranging from C4 to C14 were blended with $PC_{61}BM$, $PC_{71}BM$, and ICBA to explore fullerene intercalation previously inaccessible with polymer systems. In both $PC_{61}BM$ and $PC_{71}BM$ blended films, we observe two regimes: bimolecular crystal and amorphous intercalated. BTTT-14 to -7 show spontaneous bimolecular crystal formation while BTTT-6 to -4 exhibit a lack of thin-film microstructural order as demonstrated by GIXD and DSC. However, complete PL quenching of the amorphous blends indicates that the fullerene and dimer are also molecularly mixed. Hole-/electron-only devices were dominated by the dimensionality and crystallinity of the materials. In OFETs, the lack of crystalline order in the amorphous blend resulted in no field effect whereas the enhanced crystalline order in the bimolecular crystal improved charge transport. This work highlights the growing list of side-chain related phenomena and rational molecular design considerations essential to morphologic control of organic semiconductors.

■ ASSOCIATED CONTENT

Supporting Information

The Supporting Information is available free of charge on the ACS Publications website at DOI: 10.1021/acs.chemmater.7b04702.

Single-crystal files (CIF)
Single-crystal files (CIF)
Single-crystal files (CIF)
Single-crystal files (CIF)
Diffractograms of neat and fullerene blended films; Q_z line cuts of $PC_{71}BM$ and ICBA blends; DSC thermograms of neat materials and $PC_{61}BM$/BTTT-12, -9, -6, and -4 blends; DSC of neat dimer powders; DSC of BTTT-4/$PC_{61}BM$, $PC_{71}BM$, and ICBA; UV−vis of neat dimers in solution and thin film and $PC_{61}BM$ blended films; detailed synthesis of dimers and ^1H NMR. (PDF)

■ AUTHOR INFORMATION

Corresponding Author

*E-mail: abriseno@mail.pse.umass.edu.

ORCID

Detlef-M. Smilgies: 0000-0001-9351-581X
Alejandro L. Briseno: 0000-0003-2981-9143

Author Contributions

#These authors contributed equally (E.K.B. and B.P.C.).

Notes

The authors declare no competing financial interest.
Additional supporting research data (BTTT-6,[28] 1496599; BTTT-7, 1554560; BTTT-9, 1554561; BTTT-10, 1554562; BTTT-11, 1554563; BTTT-12[27]) for this article may be accessed at https://www.ccdc.cam.ac.uk/.

DOI: 10.1021/acs.chemmater.7b04702
Chem. Mater. XXXX, XXX, XXX−XXX

■ ACKNOWLEDGMENTS

E.K.B., B.P.C., and A.L.B. acknowledge the support of the Office of Naval Research (N000141110636, N0001471410053). This work is based upon research conducted at the Cornell High Energy Synchrotron Source (CHESS) which is supported by the National Science Foundation and the National Institutes of Health/National Institute of General Medical Sciences under NSF award DMR-1332208.

■ REFERENCES

(1) Hoppe, H.; Sariciftci, N. S. Morphology of polymer/fullerene bulk heterojunction solar cells. *J. Mater. Chem.* **2006**, *16*, 45−61.
(2) Liu, Y.; Zhao, J.; Li, Z.; Mu, C.; Ma, W.; Hu, H.; Jiang, K.; Lin, H.; Ade, H.; Yan, H. Aggregation and morphology control enables multiple cases of high-efficiency polymer solar cells. *Nat. Commun.* **2014**, *5*, 5293.
(3) Benanti, T. L.; Venkataraman, D. Organic solar cells: An overview focusing on active layer morphology. *Photosynth. Res.* **2006**, *87*, 73−81.
(4) Chen, L. M.; Hong, Z.; Li, G.; Yang, Y. Recent progress in polymer solar cells: manipulation of polymer: fullerene morphology and the formation of efficient inverted polymer solar cells. *Adv. Mater.* **2009**, *21*, 1434−1449.
(5) Collins, B. A.; Li, Z.; Tumbleston, J. R.; Gann, E.; McNeill, C. R.; Ade, H. Absolute measurement of domain composition and nanoscale size distribution explains performance in PTB7: PC71BM solar cells. *Adv. Energy Mater.* **2013**, *3*, 65−74.
(6) Yan, H.; Collins, B. A.; Gann, E.; Wang, C.; Ade, H.; McNeill, C. R. Correlating the efficiency and nanomorphology of polymer blend solar cells utilizing resonant soft X-ray scattering. *ACS Nano* **2012**, *6*, 677−688.
(7) Dennler, G.; Scharber, M. C.; Brabec, C. J. Polymer-Fullerene bulk-heterojunction solar cells. *Adv. Mater.* **2009**, *21*, 1323−1338.
(8) Yu, G.; Gao, J.; Hummelen, J. C.; Wudl, F.; Heeger, A. J. Polymer photovoltiac cells: Enhanced efficiencies via a network of internal donor-acceptor heterojunctions. *Science* **1995**, *270*, 1789.
(9) Kozub, D. R.; Vakhshouri, K.; Orme, L. M.; Wang, C.; Hexemer, A.; Gomez, E. D. Polymer crystallization of partially miscible polythiophene/fullerene mixtures controls morphology. *Macromolecules* **2011**, *44*, 5722−5726.
(10) Yin, W.; Dadmun, M. A new model for the morphology of P3HT/PCBM organic photovoltaics from small-angle neutron scattering: rivers and streams. *ACS Nano* **2011**, *5*, 4756−4768.
(11) Chen, D.; Nakahara, A.; Wei, D.; Nordlund, D.; Russell, T. P. P3HT/PCBM bulk heterojunction organic photovoltaics: correlating efficiency and morphology. *Nano Lett.* **2011**, *11*, 561−567.
(12) Treat, N. D.; Brady, M. A.; Smith, G.; Toney, M. F.; Kramer, E. J.; Hawker, C. J.; Chabinyc, M. L. Interdiffusion of PCBM and P3HT reveals miscibility in a photovoltaically active blend. *Adv. Energy Mater.* **2011**, *1*, 82−89.
(13) Collins, B. A.; Gann, E.; Guignard, L.; He, X.; McNeill, C. R.; Ade, H. Molecular miscibility of polymer− fullerene blends. *J. Phys. Chem. Lett.* **2010**, *1*, 3160−3166.
(14) Miller, N. C.; Cho, E.; Gysel, R.; Risko, C.; Coropceanu, V.; Miller, C. E.; Sweetnam, S.; Sellinger, A.; Heeney, M.; McCulloch, I.; et al. Factors governing intercalation of fullerenes and other small molecules between the side chains of semiconducting polymers used in solar cells. *Adv. Energy Mater.* **2012**, *2*, 1208−1217.
(15) Miller, N. C.; Cho, E.; Junk, M. J.; Gysel, R.; Risko, C.; Kim, D.; Sweetnam, S.; Miller, C. E.; Richter, L. J.; Kline, R. J.; et al. Use of X-Ray Diffraction, Molecular Simulations, and Spectroscopy to Determine the Molecular Packing in a Polymer-Fullerene Bimolecular Crystal. *Adv. Mater.* **2012**, *24*, 6071−6079.
(16) Miller, N. C.; Gysel, R.; Miller, C. E.; Verploegen, E.; Beiley, Z.; Heeney, M.; McCulloch, I.; Bao, Z.; Toney, M. F.; McGehee, M. D. The phase behavior of a polymer-fullerene bulk heterojunction system that contains bimolecular crystals. *J. Polym. Sci., Part B: Polym. Phys.* **2011**, *49*, 499−503.
(17) Miller, N. C.; Sweetnam, S.; Hoke, E. T.; Gysel, R.; Miller, C. E.; Bartelt, J. A.; Xie, X.; Toney, M. F.; McGehee, M. D. Molecular packing and solar cell performance in blends of polymers with a bisadduct fullerene. *Nano Lett.* **2012**, *12*, 1566−1570.
(18) Cates, N. C.; Gysel, R.; Beiley, Z.; Miller, C. E.; Toney, M. F.; Heeney, M.; McCulloch, I.; McGehee, M. D. Tuning the properties of polymer bulk heterojunction solar cells by adjusting fullerene size to control intercalation. *Nano Lett.* **2009**, *9*, 4153−4157.
(19) Mayer, A.; Toney, M. F.; Scully, S. R.; Rivnay, J.; Brabec, C. J.; Scharber, M.; Koppe, M.; Heeney, M.; McCulloch, I.; McGehee, M. D. Bimolecular crystals of fullerenes in conjugated polymers and the implications of molecular mixing for solar cells. *Adv. Funct. Mater.* **2009**, *19*, 1173−1179.
(20) Cates, N. C.; Gysel, R.; Dahl, J. E.; Sellinger, A.; McGehee, M. D. Effects of intercalation on the hole mobility of amorphous semiconducting polymer blends. *Chem. Mater.* **2010**, *22*, 3543−3548.
(21) Buchaca-Domingo, E.; Ferguson, A.; Jamieson, F.; McCarthy-Ward, T.; Shoaee, S.; Tumbleston, J.; Reid, O.; Yu, L.; Madec, M.-B.; Pfannmöller, M.; et al. Additive-assisted supramolecular manipulation of polymer: fullerene blend phase morphologies and its influence on photophysical processes. *Mater. Horiz.* **2014**, *1*, 270−279.
(22) Rance, W. L.; Ferguson, A. J.; McCarthy-Ward, T.; Heeney, M.; Ginley, D. S.; Olson, D. C.; Rumbles, G.; Kopidakis, N. Photoinduced carrier generation and decay dynamics in intercalated and non-intercalated polymer: fullerene bulk heterojunctions. *ACS Nano* **2011**, *5*, 5635−5646.
(23) Savenije, T. J.; Grzegorczyk, W. J.; Heeney, M.; Tierney, S.; McCulloch, I.; Siebbeles, L. D. Photoinduced Charge Carrier Generation in Blends of Poly (Thienothiophene) Derivatives and [6, 6]-Phenyl-C61-butyric Acid Methyl Ester: Phase Segregation versus Intercalation. *J. Phys. Chem. C* **2010**, *114*, 15116−15120.
(24) Scarongella, M.; De Jonghe-Risse, J.; Buchaca-Domingo, E.; Causa, M.; Fei, Z.; Heeney, M.; Moser, J.-E.; Stingelin, N.; Banerji, N. A close look at charge generation in polymer: fullerene blends with microstructure control. *J. Am. Chem. Soc.* **2015**, *137*, 2908−2918.
(25) Causa, M.; De Jonghe-Risse, J.; Scarongella, M.; Brauer, J. C.; Buchaca-Domingo, E.; Moser, J.-E.; Stingelin, N.; Banerji, N. The fate of electron−hole pairs in polymer: fullerene blends for organic photovoltaics. *Nat. Commun.* **2016**, *7*, 12556.
(26) Kang, K.; Watanabe, S.; Broch, K.; Sepe, A.; Brown, A.; Nasrallah, I.; Nikolka, M.; Fei, Z.; Heeney, M.; Matsumoto, D.; et al. 2D coherent charge transport in highly ordered conducting polymers doped by solid state diffusion. *Nat. Mater.* **2016**, *15*, 896−902.
(27) Zhang, L.; Liu, F.; Diao, Y.; Marsh, H. S.; Colella, N. S.; Jayaraman, A.; Russell, T. P.; Mannsfeld, S. C.; Briseno, A. L. The good host: formation of discrete one-dimensional fullerene "channels" in well-ordered Poly (2, 5-bis (3-alkylthiophen-2-yl) thieno [3, 2-b] thiophene) oligomers. *J. Am. Chem. Soc.* **2014**, *136*, 18120−18130.
(28) Cherniawski, B. P.; Lopez, S. A.; Burnett, E. K.; Yavuz, I.; Zhang, L.; Parkin, S. R.; Houk, K. N.; Briseno, A. L. The effect of hexyl side chains on molecular conformations, crystal packing, and charge transport of oligothiophenes. *J. Mater. Chem. C* **2017**, *5*, 582−588.
(29) Chabinyc, M. L.; Toney, M. F.; Kline, R. J.; McCulloch, I.; Heeney, M. X-ray scattering study of thin films of poly (2, 5-bis (3-alkylthiophen-2-yl) thieno [3, 2-b] thiophene. *J. Am. Chem. Soc.* **2007**, *129*, 3226−3237.
(30) McCulloch, I.; Heeney, M.; Bailey, C.; Genevicius, K.; MacDonald, I.; Shkunov, M.; Sparrowe, D.; Tierney, S.; Wagner, R.; Zhang, W.; et al. Liquid-crystalline semiconducting polymers with high charge-carrier mobility. *Nat. Mater.* **2006**, *5*, 328−333.
(31) Koppe, M.; Scharber, M.; Brabec, C.; Duffy, W.; Heeney, M.; McCulloch, I. Polyterthiophenes as donors for polymer solar cells. *Adv. Funct. Mater.* **2007**, *17*, 1371−1376.
(32) Hoppe, H.; Niggemann, M.; Winder, C.; Kraut, J.; Hiesgen, R.; Hinsch, A.; Meissner, D.; Sariciftci, N. S. Nanoscale morphology of conjugated polymer/fullerene-based bulk-heterojunction solar cells. *Adv. Funct. Mater.* **2004**, *14*, 1005−1011.

DOI: 10.1021/acs.chemmater.7b04702
Chem. Mater. XXXX, XXX, XXX−XXX

(33) Yu, G.; Heeger, A. J. Charge separation and photovoltaic conversion in polymer composites with internal donor/acceptor heterojunctions. *J. Appl. Phys.* **1995**, *78*, 4510−4515.
(34) Marsh, H. S.; Jayaraman, A. Effect of side chain length on the morphology of blends of 2,5-bis(3-alkylthiophen-2-yl)thieno[3,2-b]thiophene oligomers and fullerene derivatives. *J. Polym. Sci., Part B: Polym. Phys.* **2016**, *54*, 89−97.

DOI: 10.1021/acs.chemmater.7b04702
Chem. Mater. XXXX, XXX, XXX−XXX